16th Australasian Fluid Mechanics Conference
Crown Plaza, Gold Coast, Australia
2-7 December 2007

A New Internal Combustion Engine Configuration: Opposed Pistons with Crank Offset

R. Malpress and D.R. Buttsworth

Faculty of Engineering and Surveying
University of Southern Queensland, Queensland, 4350 AUSTRALIA

Abstract

Theoretical and experimental performance results for a new internal combustion engine configuration are presented in this paper. The engine is a piston ported, spark ignition petrol engine which consists of two opposed pistons in a single cylinder controlled by two synchronously timed crankshafts at opposite ends of the cylinder. It makes use of crank offset to create the required piston motion aimed at engine efficiency improvements through thermodynamic performance gains. In particular, the engine employs full expansion in which the power stroke displaces a larger volume than the compression stroke, thereby allowing the expanding gas to reach near atmospheric pressure before the exhaust port opens. This allows more work to be done by each thermodynamic cycle. It also features a greater rate of volume change after combustion than a convention 4-stroke engine for the same crank speed. This reduces the time that the temperature difference between the gas and the cylinder is high relative to a conventional engine which in turn, should reduce the heat lost from the combustion products. Thermodynamic and friction modelling of the engine indicated that efficiencies around 38% might be achieved. However, experiments with a prototype engine demonstrated that friction losses in the engine exceeded that predicted in the original modelling.

Introduction

This project is motivated by the desire to identify techniques to improve engine efficiency. Theoretical efficiency limits are far higher then those achieved by conventional engines so there should be reasonable prospects for engine efficiency improvements. Typical engine efficiency is quoted at wide open throttle (WOT) where the engine is operating at peak pressures and consequently peak thermal efficiency. For petrol engines, the WOT efficiency achieved is typically in the low to mid 30% range but the theoretical thermal efficiency of the Otto cycle is well over 50% for a compression ratio tolerated by petrol engines. For example, the theoretical thermal efficiency of an Otto cycle at a compression ratio of 10:1 is 61% (Cengel and Boles [1]).

An increasing awareness of the consequences of energy use is emerging as a contemporary social issue. It is reflected in Global Warming concerns as a consequence of Green House Gas (GHG) emissions. Internal combustion engine emissions are a significant contributor. The Australian Green House Office [2] reports that transport contributed 14% of 2005 GHG emissions in Australia. The vast majority of this was from internal combustion engine powered vehicles. 50% of total emissions in that year were reported from stationary power generation to which internal combustion engines also contribute. These figures indicate that at least one sixth of the GHG produced in Australia is from internal combustion engines.

Many government agency and corporate web sites present the sustainability of internal combustion engine fuels in varied lights. OPEC [3] countries report having added reserves in the period 2000-2005 which exceeded the cumulative production up to that time. ASPO Australia [4] reports Australian oil reserves have peaked and that it 'serves as a microcosm of a world entering the peak oil era'. Many media and web publications reflect varied opinion about the peak oil phenomenon. Most dispute arises about the extent of yet undiscovered reserves. Consistently though, the tone is that pressure is developing on the supply side resulting in expected increases in oil prices in the near future.

In spite of the mounting pressures building against the use of internal combustion engines, they dominate the automotive field. This reflects their inherent suitability based on their many favourable traits, suggesting that the prolific use of internal combustion engines will continue. Consequently, any improvements in engine efficiency will become a requirement via supply and demand economic principles and through regulatory control of emissions through the political system.

Engine efficiency is becoming a more prominent factor in automobile manufacturer's decision making. Ford Motor Company released a report [5] in 2006 outlining its approach to environmental concerns. It referred to several technological developments associated with improved efficiency and reduced emissions. Ford's CEO, Bill Ford is quoted to say, "We are more convinced than ever that our long-term success depends on how our Company addresses issues such as climate change, energy security, …, noise and innovative use of renewable resources and materials." Significant focus over recent years has lead to various technological advances in engine control resulting in efficiency gains. Features such as variable valve timing and its associated control have appeared recently in production vehicles. The preface of Variable Valve Actuation 2000 [6] refers to the predicted outcome of current variable valve timing technology to be camless valve actuation leading to efficiency improvements. In general however, little attention has been paid to engine configuration alternatives although several concepts have been developed to various extents in the past. Saab [7] researched a variable displacement engine using mechanical means to change the compression ratio. Australia's Ralph Sarich invented an engine configuration alternative, the orbital engine. The Power House Museum [8] has a site referring to the orbital engine development timelines and outcomes.

The opposed piston engine introduced in this paper is an alternative engine configuration that, through its unique engine geometry attempts to address certain deficiencies of the thermodynamic cycle as employed in conventional engines. Specifically, the new configuration adopts a full expansion that aims to extract the proportion of the energy still available in a conventional engine when the exhaust valve opens. At WOT this represents approximately 20% of the total work by the thermodynamic cycle in a conventional engine. Furthermore, via crankshaft offset (in which the crankshaft centreline is displaced from the cylinder centreline), the piston motion used in the opposed piston engine creates a faster rate of change of the engine volume after combustion thereby reducing the gas temperature in a shorter time than for an equivalent conventional

engine. This is intended to reduce convective heat losses during the power stroke, improving thermodynamic efficiency. This earlier reduction in temperature is expected to allow the engine to burn a pure charge without an increase in NO_X production. All these features are potential benefits of the engine design described in this paper.

The opposed piston engine concept is investigated in this paper through thermodynamic and friction simulations, finite element modelling of crank shaft stress, and experiments performed on a prototype configuration.

Thermodynamic Simulations

The primary simulation tool used to analyse the engine and assist in the design process was a purpose-built thermodynamic model written in Matlab. The Matlab package performs several functions including, physical parameter analysis, thermodynamic analysis, friction and other loss analysis, optimisation, and visualisation of the cycle.

The thermodynamic simulation outputs the net work done in one cycle and is the starting point for the efficiency analysis. The simulation adopts certain elements from an existing engine simulation program written by Ferguson [9] and implemented in Matlab by Buttsworth [10]. The piston cylinder is modelled as a geometric cylinder and temperature, pressure, and volume increments equivalent to one degree crankshaft rotation are used in the integration process. The simulation includes the following thermodynamic features:

- Equilibrium combustion products calculated based on temperature and pressure using the simplified approach of Olikara and Borman [11].
- Heat loss from the working gas using a user-defined heat transfer coefficient.
- Burn time set by an input constant following the approach of Ferguson [9].
- Gas loss via blow-by estimated using a first order system approximation with a user-defined rate-constant.

To readily investigate the effects of various geometric and thermodynamic model parameters on the engine performance, and to reach an optimum configuration for any desired engine output, the parameters identified in Table 1 were established in a graphical user interface (GUI). For each of these parameters, Table 1 shows the maximum, minimum and default values available through the GUI. The user then varies any of these default values in the GUI. A new thermodynamic simulation is performed whenever a new set of parameters is established.

Engine Parameter	Range	Specification (Opt. Config.)
Upper Crank Offset (mm)	-40:0.2:0	-9.2
Upper Conrod Length (mm)	40:0.2:80	50.5
Upper Crank Throw (mm)	25:0.2:50	37.1
Lower Crank Offset (mm)	-40:0.2:0	-9.2
Lower Conrod Length (mm)	40:0.2:80	48
Lower Crank Throw (mm)	25:0.2:50	36.5
Crank Separation(vertical mm)	80:0.2:100	98.5
Exhaust Port Height (mm)	10:0.2:20	12.5
Upper Crank Lag (degrees)	-10:0.02:10	6.8
Burn Start (degrees before minimum piston separation)	-50:0.02:0	-25.5
Burn Duration (degrees after Burn Start)	20:0.02:100	60

Table 1. GUI input data from specification file. Data determined from optimisation within the GUI and return to the specification file.

The thermodynamic simulation generates engine pressure and other thermodynamic properties for the cycle at each one degree increment of crankshaft rotation. These outputs are then used to calculate the connecting rod loads and resulting cylinder-to-piston reaction loads necessary in the piston friction loss calculations. Figure 1 shows the GUI output illustrating the relative position of the two pistons during one cycle.

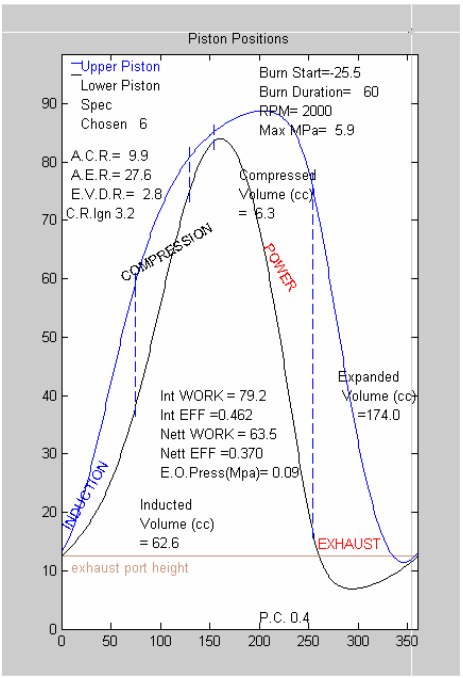

Figure 1. GUI output screen showing relative position of the two pistons (mm displacement on the vertical axis) as a function of crank angle (on the horizontal axis) and provides other numerical outputs.

Features displayed in Figure 1:

- Representations of the maximum inducted volume, minimum compressed volume, including spark plug port volume and maximum expanded volume are shown as dotted lines in their relative positions in one crankshaft rotation after the exhaust port closes.
- The relative positions of the 4 cycle phases are shown as 'INDUCTION', 'COMPRESSION', 'POWER', 'EXHAUST'. All are achieved in a single revolution of the crankshafts.
- The geometry of the engine creates the path for each piston that generates the different displacements in the induction and expansion phases. This allows for full expansion.
- The pistons are at minimum separation as their motion closes the exhaust port. This provides nearly complete scavenging.
- At maximum separation at the end of induction, the induction port is closed and the compression phase commences.
- Ignition occurs earlier than minimum separation in the compression phase. The model predicts the optimum ignition point by iterative calculations of user inputs aiming for optimum efficiency.
- After minimum separation the upper piston is still moving up and the lower piston begins moving down giving the fast expansion phase during the power stroke resulting in reduced thermal losses through a reduced temperature difference between the wall and the gas.

- The power stroke continues until the maximum expanded volume. Optimisation moved this point as close as possible to the exhaust port opening. While the lower piston opens the exhaust port, the upper piston moves down exhausting the chamber. The two piston then approach minimum separation as they pass the top of the exhaust port while both are moving up.
- The cycle is completed in one revolution.
- Table 2 shows the numeric data displayed in Figure 1.

Engine Specification file	enginespecoptsizechosen 6
Burn Start (degrees before minimum piston separation)	25.5
Burn Duration (degrees after Burn Start)	60
Engine Speed (rpm)	2000
Maximum Engine Pressure (MPa)	5.9
Actual Compression Ratio (A.C.R.)	9.9:1
Actual Expansion Ratio (A.E.R.)	27.6:1
Effective Variable Displacement Ratio (E.V.D.R)=(A.E.R.)/(A.C.R.)	2.8
Inducted Volume (cm^3)	62.6
Compressed Volume (Minimum piston separation during burn) (cm^3)	5.3
Expanded Volume (cm^3)	174.0
Thermodynamic Work (J/cycle)	79.2
Thermodynamic cycle efficiency (modelled) (%)	46.2
Net Work (Thermodynamic work – losses) (J/cycle)	63.5
Net Efficiency (%)	37.0
Exhaust opening Pressure (MPa)	0.09

Table 2. GUI/model output data as displayed in Figure 1 for the original Matlab optimised configuration.

Figure 2 shows what the model predicts for the work accumulated through the thermodynamic cycle for the opposed piston engine in comparison to the engine modelled by Ferguson [9].

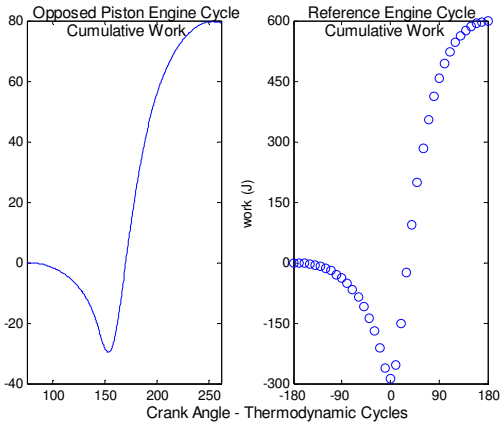

Figure 2. Matlab model plot of comparison between thermodynamic cycle work of the opposed piston engine and a reference engine.

As necessary for the opposed piston cycle to be more efficient, the proportion of compression work over the total work is smaller than in the conventional engine.

Other engine characteristic input specifications are read from a separate file that specifies parameters such as engine speed, spark plug chamber volume, oil viscosity and the parameters needed to complete the thermocycle modelling. Changing the engine speed in the model resulted in the following changes to net efficiency.

Engine Speed (rpm)	Net Efficiency (%)
1000	32.7
2000	37.0
3000	33.4
4000	24.9

Table 3. Comparison of Net efficiencies at various engine speeds.

The Net efficiency varies considerably over a range of typical engine speeds. The maximum net efficiency is achieved at about 2000 rpm. Lower speeds have reduced thermodynamic cycle performance. As speed increases above 2000 rpm, losses increase at an increasing rate. The result is expected because of the dynamic effect of piston friction due to the high conrod angles required as a consequence of crankshaft offset.

The consequence of various inputs changes can be visualised with reference to Figure 1. Reducing the crankshaft lag shifts the lower piston plot to the left relative to the upper piston and consequently the pistons would interfere unless the crank shaft separation is increased. This results in a net decrease in the compression ratio and an increase in the E.V.D.R. (see Table 2.). The maximum compression ratio considered in the model is 10:1 reflecting the knock limits for petrol.

The primary goal is maximum efficiency. A variation to any input specification changes the output. The initial Matlab model of Figure 1 has optimised the net efficiency for a compression ratio near 10:1. The geometry and associated specifications were shown to be impractical to build (refer to the section, Engine Configuration and Features). Consequently the optimum Matlab model configuration was not able to be attained. A new optimum net efficiency was obtained from the model under the restricted conditions of the engine specifications that were possible to build. Table 4 shows that the net efficiency, compression ratio and net work per cycle for these two engine specifications and for the specifications achieved in the prototype (see Engine Configuration and Features). The net efficiency, the prime objective, necessarily fell as it had in each previous condition been optimised.

Engine Specification (2000 rpm)	Net Efficiency (%)	Compression Ratio	Net work per cycle (J)
Optimised original configuration	37	9.9:1	63.5
Modified by build restrictions	33.4	8.6:1	28.7
prototype	30.2	4.2:1	22.2

Table 4. Comparison of engine outputs for the engine specification under three conditions

Friction and other Losses

The net efficiency is the internal thermodynamic work done by the engine cycle less the losses due to friction, pumping and ancillaries load. The friction includes the piston, ring and bearing friction. Pumping losses define the work required to transport the inducted gas into the engine and expel the burnt gas. Ancillary

losses are restricted to the synchronous belt drive required to maintain the engine's two crankshafts.

The losses model features:

- Ring friction
- Piston friction including dynamic effects and reaction loads
- Friction based on Stribeck theory
- pumping losses
- bearing and belt losses

The piston friction model is also implemented in Matlab and considers the loads and reactions within the engine based on a dynamic analysis for the two pistons at one degree of crankshaft rotation iterations at the design speed and pressure loading derived from the thermodynamic simulation. It assumes the rotational momentum of the connecting rod to be negligible. Coefficient of friction data necessary in these simulations is derived from the Stribeck diagram of Stone [12]. Figure 3 depicts the relationship between viscosity, velocity, pressure and coefficient of friction for bearing surfaces in a typical engine. The friction model employed a value of viscosity which equated to the general data for SAE 50 oil at 120°C. The engine inducts oil and operates with 2-stroke oil in the crank cases.

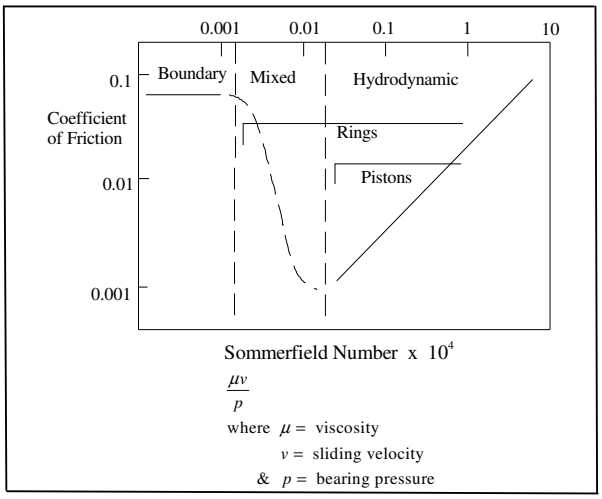

Figure 3. Engine lubrication regimes defined in the Stribeck diagram. The diagram reflects the general nature of engine friction. Only the piston skirts operate in full hydrodynamic conditions in conventional engines referred to here. Adapted from Stone [12]

Figure 4 shows a plot of the piston friction regime for the prototype. It reveals that the engine configuration shifts the piston skirt friction into the mixed regime with some boundary friction, which is not usually experienced in conventional engines.

The data shown in Figure 4 is generated by the Matlab model with the calculations refined from information obtained from the prototype tests (see Prototype Test Results and Analysis). Only a small portion of the cycle is in full hydrodynamic lubrication (dotted plot). The majority of the cycle is in the mixed friction regime of Figure 3. The plot is configured to display the maximum friction for all configurations. The small proportion of the vertical scale occupied shows that the friction is low for this configuration relative to other engine configurations modelled. The discontinuities at approximately 150 and 315 degrees are the change of direction points for the piston motion. The discontinuity at approximately 250 degrees is the point where the conrod load reverses from accelerating the piston to decelerating the piston.

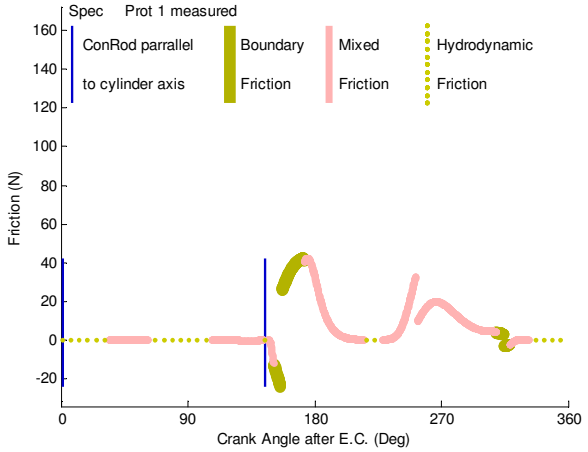

Figure 4. Piston friction modelled forces as a function of crank angle after E.C. and engine lubrication regimes defined in the Stribeck diagram for the lower piston for the prototype operated at 2000rpm producing a maximum engine pressure of 0.9MPa, net work per cycle of 17.4J with net efficiency of 23.3%.

Engine Configuration and Features

For the engine configuration, the Matlab model simply defined the displaced volume and piston position required to create the engine cycle which reflected the initial concept. Once the Matlab model produced engine specifications, the prototype was modelled in ProEngineer solid modelling package.

The first benefit of this process came when the selected optimum configuration proved to be impossible to construct. The interference resulting from the low connecting rod/crank throw ratio resulted in too little room for sufficient material in the cylinder walls at the extreme piston position to adequately support the piston. No combination of crank throw and cylinder wall arrangements was feasible. Consequently, the Matlab model was employed to reconstruct the engine specifications with an increased connecting rod length. The resulting net efficiency necessarily decreased as it had been previously optimised. The loss in efficiency was approximately 2.6% net (see Table 4). Figure 5 is an engine drawing using the model reconstructed engine specifications.

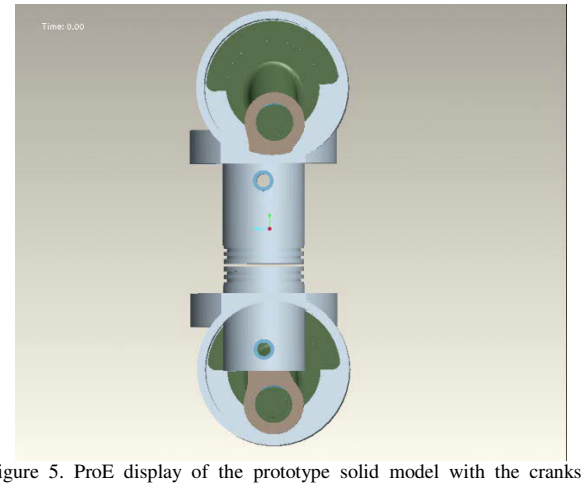

Figure 5. ProE display of the prototype solid model with the cranks located at a position just before the start of the induction stroke – crankshafts rotate clockwise as viewed. The image shows that the upper crank lags the lower crank by a few degrees. Crank offsets results in asymmetric piston motion between the 'up' and 'down' strokes creating the displacement depicted in Figure 1.

At this stage, the details for the engine components and their specification became necessary. The exhaust port position was established by the thermodynamic simulations. An original intention to arrange the induction through a poppet valve in the lower cylinder was abandoned and replaced by a reed valve controlled induction port in the cylinder wall. The main bearings were chosen as deep groove ball bearings with the outer bearings having an integral seal. Needle roller bearings used in a production 2-stroke mower engine were selected for the connecting rods. The crankshaft is supported on one side only allowing the big end roller bearing to be assembled by screwing in the crank pin from the same production engine. The crank timing is achieved with a synchronous belt drive and idler tensioner. Carburation and ignition was arranged as required from off the shelf and available components. The engine is fitted with two spark plugs at approximately opposite sides of the cylinder.

Figure 6 is a photograph of the prototype prior to testing. In this arrangement the 12V starter motor is fitted. The engine has been laid down to the right. The lower case of Figure 5 is on the left in Figure 6.

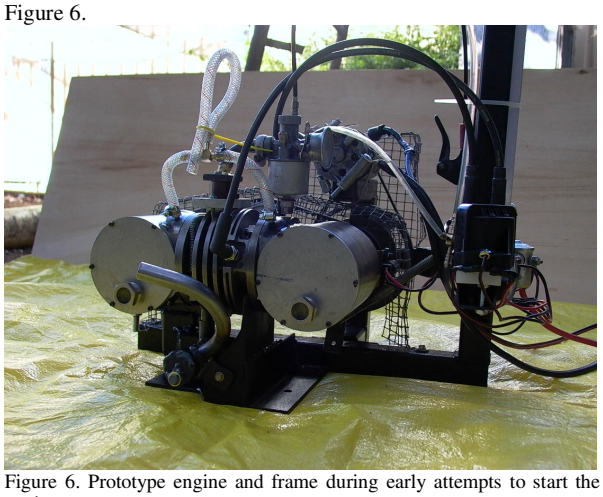

Figure 6. Prototype engine and frame during early attempts to start the engine

FEA used to specify critical components

The two complicated parts of the engine that differ substantially from a conventional engine and therefore required stress analysis are the pistons and cranks. Each piston is essentially the same, though one uses three compression rings and the other uses two. This was necessary to maintain at least one ring seal as the pistons moved past the spark plug port during compression and 2 ring seals to hold the combustion pressure. The two crankshafts are the same, except for a slightly different throw.

The thermodynamic model was used to define the loads and the solid models define the geometry. A finite element analysis (FEA) package (Ansys Ed Release 10) was used to assess the maximum stress and in particular, the predicted fatigue life. The prototype was designed to operate for sufficient time to produce usable performance data.

Figure 7 shows another plot produced by the thermodynamic model. This plot gives the relative angle between the connecting rod and the crank throw. Assuming essentially no friction at the big-end (the needle roller bearing) and negligible conrod weight, Figure 7 defines the load direction for the finite element analysis. The plot positions the connecting rod load, also determined in the thermodynamic model, so as too assess the load to apply in the FEA.

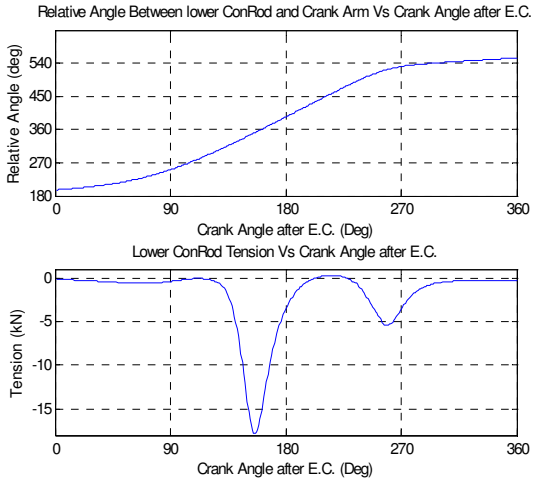

Figure 7. Thermodynamic model results used to specify the FEA loads.

Figure 8 shows a graphical display of the stress on the crankshaft under the loads determined by the Matlab model. The unusual inclined crank arm is necessary to allow the piston crankcase and cylinder to operate effectively. It results in a significant bending in the crank when loaded and as a result the inner bearing is much larger than that for an equivalent conventional engine.

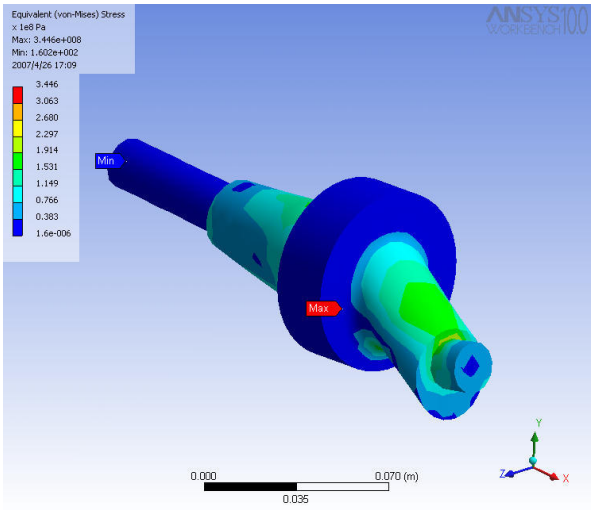

Figure 8. FEA stress contour plots of the crankshaft

Initial Testing and Refinement of Prototype

The dimensions of certain components were unfortunately out of tolerance, so the prototype would not accurately reflect the Matlab model used to create the engine specification. In particular, the crankshaft throws differed sufficiently to reduce the compression ratio from the initial design value of 8.6:1 to an as-constructed value of 5.1:1. Actual prototype dimensions were taken and returned to the thermodynamic model to calculate a new efficiency.

The first attempt to start the engine was unsuccessful. The engine was initially fitted with a modified 2-stroke mower pull starter. It produced about three revolutions of motion from a single pull. The high friction of the engine assembly relative to its angular momentum resulted in a small number of starting cycles at a low speed in any one attempt. Infrequent burning resulted. Several

barriers to successful engine starting became apparent. These barriers are summarised below.

- The pistons rings are conventional 2-stroke rings and were not intended for, or capable of, excluding crankcase oil from the combustion chamber. Without being able to get the engine spinning for sufficient time to bed the rings and without sufficiently frequent ignition and burning, oil accumulated in the combustion chamber and frequently bridged the spark gap.
- The inducted gas flow was very slow and the carburettor metering of the mixture at those flows could not be confirmed. It could not be assessed if the poor ignition and burn was a result of a poor mixture.
- It could not be assessed whether a single ignition and burn had some dynamic effect on the next inducted charge causing the infrequent burn.

Efforts to address the burn problems included:

- Engine pre-heat by a fan heater. The engine external temperature exceeded 100^{o}C (water droplet test).
- Powering the engine with a small 12V starter motor. However, the length of time in cranking mode without ignition exceeded the starter motor's duty cycle.
- Mixture control, initially achieved with carburettor choking. However, the engine continued to suffer from poor and inconsistent burn, so later, the fuel to air ratio was also made externally adjustable at the main jet in the carburettor.
- Combustion chamber shape changes attempting to improve flame propagation were achieved by machining the crowns of the pistons. Figure 9 shows photographs of the piston before and after the piston crown changes. The u-shaped grooves were approximately 10mm wide and 3mm deep. This was an attempt to allow the burn to penetrate the gap between the pistons.

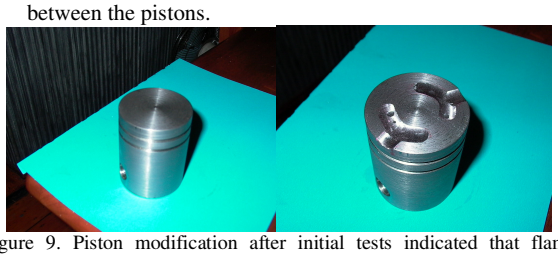

Figure 9. Piston modification after initial tests indicated that flame propagation was a problem

Finally, an electric motor was arranged to motor the engine at reasonable speeds and for periods sufficient to enable measurements of inducted air flow speed, fuel flow rate, engine speed and input torque. These measurements facilitated subsequent analysis of the engine's performance.

The inconsistent burn problem persisted and was also addressed by the addition of multiple sparks during the expected burn period. Of all the modifications employed, the addition of multiple sparks made the most significant improvement to the burn. The engine was built with two spark plug ports on approximately opposite sides of the cylinder. This was done to provide a mechanism to assess the effect on efficiency of the spark initiating burn from one side of the narrow disk shaped combustion chamber in comparison to a burn simultaneously initiated from opposite sides of the combustion chamber. All reference to ignition and burn in this paper are for both spark plugs firing at the same time. The reason multiple sparks resulted in a more complete burn could be related to the speed and direction of the gas flow as both pistons move past the spark plug port. Prior to minimum separation of the pistons in the compressed positions the speed of the gas being 'squished' into the spark plug ports could exceed the flame speed in the conditions. The very small combustion volume with intruding edges and complex fluid motion is likely responsible. A very poor burn was achieved in many configurations of ignition timing, mixture, engine speed and engine temperature prior to the addition of multiple sparks. As the overall burn is improved by subsequent sparks, it is clear that there is a flame propagation problem in the prototype configuration. The prospect for a complete burn is low even with multiple sparks because the probability of a combustible pocket of gas existing at the spark plug ports diminishes with each subsequent spark-combustion event.

Prototype Test Results and Analysis

Table 5 shows data taken after the engine had operated for a total of approximately one hour in various conditions. Initial motoring torques were higher than that indicated in Table 5. This was mostly due to the running in period for all engine components, in particular, the bearings and rings.

The inducted air flow was measured in the tube upstream of the carburettor using a Pitot tube coupled to an inclined, ethanol-filled manometer. The fuel flow rate was measured by timing the fuel level drop in a vertical tube with internal diameter resulting in 55 mm/cm^3. The motor torque measurement was via a spring balance over a 0.180m arm. The engine did not produce sufficient thermodynamic work to overcome engine friction, but measurement of the contribution of the thermodynamic work could be obtained from the reduction in the input power of the motoring electric drill when the engine ignition was switched on.

Test	Ignit.	Inclined Manometer		Engine Speed (rpm)	Torque	Fuel	
		Angle (deg)	Deflect. (mm)		Spring Force (kg)	Δh (mm)	time (s)
1	No	5	12	1050	3		
	No	5	10	920	3.6		
	Yes	5	6	1440	2.1	190	16.3
2	No	3	25	1100	2.7		
	No	3	22	970	2.6		
	Yes	3	24	1320	1.7	180	13.6
	Yes	3	20	1430	1.4	180	13.6
3	No	3	20	1120	2.2		
	Yes	3	24	1400	1.5	220	15

Table 5. Motoring test data. Data from three tests performed over two days are presented.

Ignit.	Pitot Δp (Pa)	Induct Air per rev (cm3)	Air Mass per rev (g)	Eng rpm	T (Nm)	Drll Work IN per rev (J)	Therm Work per (J)	Fuel Mass per rev (g)	Air/ Fuel mass ratio
Test 1									
No	9.4	117		1050	5.3	33			
No	7.8	121		920	6.4	40			
Yes	4.7	60	0.073	1440	3.7	23	13	0.006	11.5
Test 2									
No	12.8	130		1100	4.8	30			
No	11.3	138		970	4.6	29			
Yes	12.3	106	0.128	1320	3	19	11	0.008	16.3
Yes	10.3	89	0.109	1430	2.5	16	14	0.007	15.0
Test 2									
No	10.3	115	0.140	1120	3.9	24			
Yes	12.3	100	0.122	1400	2.6	17	8	0.008	14.8

Table 6. Motoring tests – derived results. Results from three tests performed over two days are presented.

Table 6 shows parameter values derived from the data presented in Table 5. The mixtures used in each test were set to the mixture that produced the highest engine speed with the ignition on. The closeness of the calculated air to fuel ratio (Table 6) to that of a typical optimum mixture indicates that the fuel and air flow measuring devices are acceptable. This implies the air flow rate results are probably reliable and thus the inducted volume per cycle is also reliably reported.

The data was measured to an accuracy that gives a general representation of the contributing effects. No error analysis was performed on the data. Future testing is planned to accurately specify the performance characterised shown in Table 5.

	Simulation	Prototype Test
Internal Work (Thermo Work) (J)	23.5	11.5 (average)
Internal Efficiency (Thermo Eff) (%)	31.4	
Net Work (J)	20.3	-19.7
Net Eff (%)	27.1	
Inducted Volume (cm^3)	27.3	94 (average)

Table 7. Comparison of simulation results and prototype test results

Table 7 provides a comparison of the simulated results for the tested prototype configuration and the experimental results. The prototype test thermodynamic work was based on the average total work input calculated from the input speed and torque for the engine being motored with ignition off less the work measured with the ignition on for each test. This represents the thermodynamic work if the friction losses are the same in both cases. This technique is used in conventional engine assessments based on the assertion that the friction losses are not significantly influenced by engine pressure.

This engine configuration inherently requires a very large conrod inclination to produce the required piston motion. That large conrod angle preoccupied the considerations for friction losses because it was anticipated that the reaction loads would result in large piston friction loads. The large conrod angle also suggests that the difference in friction loss between the motored engine and the engine with ignition and burn might be more significant than they would be in a conventional engine. Consequently, the 11.5 J of thermodynamic work calculated from the engine test would be conservative. In spite of this, there still remains a significant difference between the modelled thermodynamic work and the estimated thermodynamic work from the test.

The most revealing consequence of the test results is that independent of whether the thermodynamic cycle could or was making the 12 J of work shown to be in deficit, the friction losses are overwhelmingly large and show no correlation to the modelled friction losses. If the engine could be coaxed into doubling its thermo work output, it could still not power itself, let alone produce any output power.

Once the engine showed such poor characteristics, a measurement of compression pressure was performed, yielding the data displayed in Table 8. The test pressure gauge was screwed into one of the spark plug ports and fitted with a non-return valve in the tip to improve the accuracy of the measurement of the actual engine pressure. The pressure fitting had similar dimensions to the spark plugs.

Engine Speed (rpm)	Compression Pressure (kPa)
400	120
500	150
600	150
700	180
800	200
860	225

Table 8. Motoring compression pressures at varying speeds

The strong relation between the compression pressure and the engine speed suggests that blow-by was very significant. The arrangement of the rings mentioned earlier was a necessary consequence of the pistons passing the spark plug ports. The spark plug ports exposed the upper cylinder upper ring directly to the compression pressure at mid compression stroke. Ring end gap was probably excessive, motivated by an expectation that the rings would be exposed to higher than normal temperatures because of the use of steel as the piston material. Steel was used because appropriate aluminium wrought bar suitable to machine the pistons was not available. This could have also resulted in a poorer seal between the ring and the hard steel groove land than would be achieved with a softer aluminium piston. Significantly, the compressed volume is exposed to ring seals on two sides unlike a conventional engine. The piston diameter is also very large relative to the compressed volume. In total, the blow-by would have significantly contributed to a reduction in the net charge available to the thermodynamic cycle.

Discussion and Implications

The initial intention of this work was to assess the potential for internal combustion engine efficiency improvement and in particular, to assess the concept engine created. The prototype test results reveal that significant deficiencies exist in the simulation model.

To more accurately assess what the engine thermodynamic cycle is achieving would require more thorough measurements and analysis of the engine performance. In particular, in-cylinder pressure measurements and/or exhaust gas measurements would need to be obtained in an effort to assess the completeness of burn in the cycle. The engine reached temperatures during the test that would equate to the temperature expected in an operating conventional engine. Significant burning was occurring.

Table 7 shows that the inducted volume per cycle on the prototype test was far higher than the engine's simulated or geometrically-identified displaced volume. The intended design had a simulated exhaust opening pressure of 90 kPa (absolute), which is the pressure at the end of the power stroke. However, the fabrication errors in the tested prototype resulted in a substantially sub-atmospheric simulated exhaust opening pressure of 50 kPa (absolute). Once the excessive blow-by and probably less then 100% burn achieved in the prototype test is taken into account, the expanding gas in the power stroke cannot fill the expanded volume of the engine and the engine consequently inducts more new charge into the engine while the engine is expanding past the induction port. The original modelling showed that a higher than atmospheric pressure was maintained over the induction port during the power stroke, thereby keeping the reed valve at the induction port closed and separating the two parts of the cycle. Because a volume similar to three times the inducted volume is inducted per cycle in the prototype test, it can be concluded that the expansion during the power stroke is only similar in volume to the inducted stroke. This means that the engine has extremely poor ring seal

characteristic and is likely to be burning less than the full charge. This easily accounts for the low thermodynamic cycle work values obtained.

The engine was disassembled and one crankshaft was motored in its case without a piston attached. The motoring torque when adjusted to match the test speeds was assessed as approximately 0.9 Nm, which represented about one third of the total motoring friction of the prototype test. This was for one crankshaft alone. The engine was further disassembled and the outer main bearings were discovered to be very 'tight', easily responsible for the majority of the measured friction on the crankshaft.

At this stage, the original simulations were reassessed and a number of significant flaws were identified.

- The thermodynamic cycle model failed to accurately account for the exposure of the spark plug ports during the compression stroke even though it was intended. The volume of the spark plug ports was not accurately included in the compression simulation, resulting in too high initial pressure for the combustion simulation. The result was an overestimate of the potential thermodynamic work in the original model. The corrected model indicates this reduces the thermodynamic work by approximately 10% from the original model predictions.
- Blow-by was accounted for and included an estimate based on doubling the blow-by included in the original thermodynamic engine simulation. This figure was evidently too low as described earlier in Prototype Test Results and Analysis. This also resulted in an overestimate of the potential thermodynamic work in the original model.
- The original Matlab model assessed the ring friction for each piston, but failed to include the total number of rings for the passive effect of ring tension and only applied the dynamic effect of engine pressure to the top ring of each piston. Blow-by would have resulted in higher ring friction due to higher pressures on outer rings then initially estimated by the model. The result was an underestimate of ring friction in the original model.
- It was assumed the largest potential for friction losses error to come from the high normal reaction loads due to the high connecting rod inclination angles. This was modelled thoroughly but no direct assessment of its accuracy is possible from the test results to this time. The piston friction could be higher than defined by the model.
- The single most deficient model characteristic was the bearing and belt friction losses. An idler tensioner was also required in the belt drive, not originally included in the model. The bearing sizes were similar to those of an engine that match the piston size and consequently the maximum piston forces. The Matlab model used a generic proportion of total engine losses as the criteria for the net bearing losses but applied it to the total thermodynamic output and not to the thermodynamic output from an engine using similar sized components. Conventional engines using components of the size used in the concept engine develop about 3 kW for the speed at which the prototype was tested. The thermodynamic cycle model indicated that the prototype would produce about 23 J of work at 2000 rpm or about 750W. This deficiency of a factor of four was a significant error and is the biggest contributor to the underestimate in total friction

Conclusions

It should be remembered that the prototype tested had specifications, resulting from fabrication errors, which produced potential performance figures significantly lower then the optimum identified from the simulations. The initial goal of the project was to assess the potential for improved internal combustion engine efficiency and in particular, the efficiency of the design concept. The prototype testing to date showed that the design concept, although capable of replicating the intended thermodynamic cycle, is unlikely to produce a functional engine with the efficiency initially predicted by the Matlab model. The Matlab model was revised with minor changes to its structure and modified parameters assessed from the prototype test. The revised Matlab model indicates that a functional engine of the design presented is possible, but could not operate at the efficiency initially predicted. The revised model predicts the engine would also operate at efficiency lower than a conventional engine. The engine's thermodynamic cycle performance has potential, but is yet to be verified by testing. The prototype test shows that the physical concept used to achieve the thermodynamic cycle does not make use of that thermodynamic cycle in an optimal fashion.

Further work and analysis on the engine is anticipated with the goal of addressing the friction and in particular refining friction analysis in the model. This will allow for a more accurate determination of performance of other aspects of the Matlab model.

Future work could address the thermodynamic deficiencies and reduce friction, but the engine shows little potential as a viable design alternative to conventional engines. The opposed piston engine concept shows potential as a research engine providing a platform for thermodynamic, combustion and friction research. The Matlab model and thermodynamic cycle have positive attributes as quantified by the engine test. They may have future applications.

References

[1] Y.A. Cengal, M.A. Boles, *Thermodynamics An Engineering Approack Fifth Edition in SI Unit,* McGraw-Hill, New York, 2006

[2] http://www.greenhouse.gov.au/inventory/2005/index.html

[3] http://www.opec.org/home/PowerPoint/Reserves/World%20crude%20oil%20reserves.htm

[4] http://www.aspo-australia.org.au/

[5] http://www.ford.com/doc/2005-06_sustainability_report.pdf

[6] *Variable Valve Actuation*, SP-1523, SAE International, Warrendale, PA, 2000

[7] http://www.fs.isy.liu.se/Lab/SVC/

[8] http://www.powerhousemuseum.com/australia_innovates/?behaviour=view_article&Section_id=1020&article_id=10041

[9] C.R. Ferguson, *Internal Combustion Engines, Applied Thernodynamics*, John Wiley and Sons, New York, 1986.

[10] Buttsworth, D. R., Spark Ignition Internal Combustion Engine Modelling using Matlab, Faculty of Engineering & Surveying Technical Reports, TR-2002-02, October 16, 2002

[11] C. Olikara and G.L. Borman, "Calculating Properties of Equilibrium Combustion Products with Some Applications to I.C. Engines", SAE Paper 750468, 1975.

[12] Stone, Richard, *Introduction to internal combustion engines*, Society of Automotive Engineers, Warrendale, Pa., c1999.